JOINT EUROPEAN TORUS JET

JET–P(93)84

A. Taroni, M. Erba, E. Springmann, F. Tibone

Global and Local Energy Confinement Properties of Simple Transport Coefficients of the Bohm Type

Global and Local Energy Confinement Properties of Simple Transport Coefficients of the Bohm Type

A. Taroni, M. Erba[1], E. Springmann, F. Tibone

JET-Joint Undertaking, Culham Science Centre, OX14 3DB, Abingdon, UK

[1]On leave from Scuola Normale Superiore, P.za dei Cavalieri, Pisa, Italy.

Preprint of a paper to be submitted for publication in
Plasma Physics and Controlled Fusion
October 1993

ABSTRACT

Global and local energy transport analysis of experimental results in TFTR and JET indicate that transport models of the Bohm type allow a better representation of experimental data than models of the gyro-Bohm type. Hence a Bohm-like model has been developed by allowing a dependence on a few dimensionless parameters so as to reproduce the main features of global L-mode thermal confinement scaling laws in Tokamaks and to obtain bowl-shaped thermal diffusivity profiles. The electron temperature profiles predicted by this model are shown to be in agreement with measured ones in a variety of steady state and time dependent JET L-mode discharges.

1. INTRODUCTION

Dimensional analysis requires that the coefficients of thermal and particle diffusion in plasmas are written as the product of a combination of local plasma variables which must produce the correct dimensions $[l^2\, t^{-1}]$, and a function of properly chosen local dimensionless plasma quantities [1], [2].

For example in the case of the thermal diffusion coefficient χ one can write:

$$\chi=\chi_0\, F(x_1,x_2,x_3...) \qquad (1)$$

where χ_0 is some basic transport coefficient (classical, neoclassical, Bohm...), and x_1,x_2,x_3 are local dimensionless parameters. The so called Kadomtsev constraint [1] verified experimentally for global confinement data in the ITER database [3], implies that the Debye length does not play a role in the definition of the dimensionless quantities. While respecting this constraint, one can shift from one definition of χ_0 to another by changing the function F.

For a chosen χ_0, only a complete determination of the function F specifies the scaling of energy confinement with respect to "engineering" parameters such as the plasma current , dimensions, input power, particle density and toroidal magnetic field, in the ideal case when other effects such as sawtooth activity, radial distribution of power sources and radiation losses do not play an important role in the global plasma energy balance.

Thus the study of anomalous energy transport in Tokamaks can be regarded as the attempt to determine the function F and its arguments for a given convenient choice of χ_0.

A choice of χ_0 is "convenient" if:

a) it is related to natural scale size and time scale of microinstabilities that are shown by theory to be possibly responsible for anomalous transport.

b) experiments can be set up for which the variables $x_1, x_2, x_3 \ldots$ can be varied independently. Such experiments allow in principle a determination of the functional dependence of χ, and their results can also be used in extrapolations to a device like ITER from present day large tokamaks, following the so-called "wind tunnel" approach [4].

As discussed in several papers starting from [1] and most recently in [5] , a proper choice of the leading term in eq.(1) is a Bohm coefficient $\chi_0 = \chi_B \propto \frac{T}{B}$.

Here T is either T_e or T_i (we choose, when required, the electron temperature T_e).

The toroidal magnetic field, $B_0 \approx |B|$, is a proper choice as a reference magnetic field, but one can introduce the poloidal field B_p by allowing an additional dependence on the safety factor q.

An important theoretical and experimental problem is to determine the dependence of F on the normalized gyroradius $\rho^* \equiv (m_i / e)^{1/2} \frac{T_e^{1/2}}{aB}$. In the case that F depends linearly on ρ^* the spatial scale of the turbulence causing transport is of the order of the gyroradius.

Then transport is determined by short wave-length turbulence and is called of the gyro-Bohm type.

On the other hand, in the case that the cell size of the turbulence causing transport scales with the machine size, F does not depend on ρ^* and transport is called of the Bohm type.

Recent results of local and global transport analysis of ad hoc experiments in TFTR [5] and JET [6] indicate that energy transport shows Bohm type rather than gyro-Bohm type features.

We start from these results as a working hypothesis and use what has become conventional terminology, stressing however that a coefficient of the Bohm or gyro-Bohm type may produce, via the functional dependences in F, an energy confinement scaling on the plasma engineering parameters that is different from that predicted by $\chi=\chi_B$ (pure Bohm) or $\chi=\chi_B\cdot\rho^*$ (pure gyro-Bohm).

We identify a family of simple functions F leading to local coefficients of thermal diffusivity of the Bohm type, that is consistent with results found so far from energy transport analysis of the so called L-mode regime in the JET Tokamak.

Most of what follows applies to both the electron and ion energy loss channel, if they are equally important in determining the plasma energy confinement properties. Alternatively, it can be applied to the loss channel that determines confinement. However, the results of numerical simulations reported here have been obtained assuming equal electron and ion thermal diffusivities, $\chi_e=\chi_i$.

2. A FAMILY OF BOHM-TYPE THERMAL DIFFUSIVITY COEFFICIENTS.

Assuming that the local energy transport coefficient is of the Bohm type we write eq.(1) as:

$$\chi = \chi_B F \propto (T / B_0)\, F\left(\nu^*, \beta_p, q, L_T^*, L_p^* \ldots\right) \qquad (2)$$

excluding explicitly a dependence of F on ρ^*. In principle the function F can depend on at least 17 non dimensional quantities [5] such as the effective collisionality parameter $\nu^* = (R/r)^{3/2} qR\nu_e (m_e / 2T_e)^{1/2}, \nu_e \propto n_e / T_e^{3/2}$ being the electron-ion collision frequency), the plasma beta $\beta = 8\pi p / B_0^2$, the safety factor q (defined via the poloidal and toroidal magnetic fluxes), the normalised scale length of variation of plasma parameters in the direction normal to the flux surfaces, e.g for the temperature $L_T^* = (dT/dr)^{-1} T / a^*$ and for the pressure $L_p^* = (dp/dr)^{-1} p / a^*$.

The normalization length a* should be related to the scale length of the saturated turbulence causing the anomaluos transport.

Our objective is to determine empirically a function F in eq.(2) leading to a coefficient χ having the properties required to simulate the temperature profiles observed in experiments. This means that χ should imply a global energy confinement scaling consistent with the results of global energy transport analysis [7,8] while at the same time it should be 'bowl shaped', increasing towards the plasma boundary. It should also provide the degree of "resilience" of the electron temperature profiles observed in L-mode discharges. Finally, the dependence of χ on the current density distribution should imply the favourable dependence of the global energy confinement on the internal inductance l_i reported for most tokamaks.

These requirements are clearly not enough to determine uniquely a transport model. However one can restrict the number of possible choices of the function F by keeping it as simple as possible and including a minimal number of non dimensional parameters with a dependence that can be tested against well diagnosed experiments set up to study particular features of L-mode confinement.

We found that a very simple expression of F leading to χ having the required properties is given by :

$$F = \alpha q^2 / \left|L_T^*\right| \tag{4}$$

where α is a numerical constant to be derived from the analysis of experimental results.

This expression gives:

$$\chi = \alpha\, \chi_B\, q^2 / \left|L_T^*\right| \propto \alpha |\nabla T| a^* q^2 / B_0 \tag{5}$$

L_T^* might equally well be replaced by L_p^* in eq. (4). Then :

$$\chi \propto \alpha |\nabla p| a^* q^2 / (B_0 n) \tag{6}$$

Eq. (6) (and similarly eq.(5)) can be rewritten in terms of a diamagnetic velocity v_d:

$$\chi \propto |v_d| a^* q^2 \,. \tag{7a}$$

This can be compared with the expression given in [4] in terms of $|v_d|$, a turbulence step size Δ and a form factor G depending on the dimensionless parameters:

$$\chi \propto |v_d| \cdot \Delta \cdot G \tag{7b}$$

In our model $\Delta \propto a^*$, $G \propto q^2$.

We assume $a^* \propto a$ or $a^* \propto q/|\nabla q|$. In steady state $q/|\nabla q| \propto a$ so that no significant difference in the scaling of energy confinement time is expected from either choice of a^*: both correspond to transport being determined by long wavelength turbulence phenomena [4],[5].

The q^2 dependence of χ implies an effective linear q dependence of the local and global energy confinement properties of the coefficient when the non linearity introduced by ∇T is taken into account. This agrees with results of the transport analysis of current ramp experiments in JET [9].

The ∇T dependence is compatible with transport studies of on/off-axis experiments in JET [10] and implies a power degradation of global energy confinement in agreement with experimental observations. A similar degradation of confinement could be obtained with a T dependence of χ, however ∇T presents some advantages. Its radial variation poses less problems than the radial variation of T, in particular it does not imply a confinement degradation when a temperature pedestal is formed at the plasma edge. In addition it implies an enhancement of χ derived from measurements of heat pulse propagation with respect to χ derived from power balance, of a factor close to two. This is consistent with results of recent analysis in JET of heat pulse propagation [11].

We notice also that the additional shear dependence introduced by $a^* \propto q/|\nabla q|$ would provide a non zero value of χ at the magnetic axis, and $\chi \Rightarrow 0$ at the separatrix of a magnetic configuration with X-points, similarily to the model of Rebut, Lallia and Watkins [12]. An increase in the local shear could then in principle counteract locally the effect of an increase in $|\nabla T|$ or $|\nabla p|/n$, compatibly with the existence of an edge pedestal in H-modes.

Such a shear dependence would remain consistent with results of current ramp experiments in JET [9] and perhaps more in line with results of current ramp experiments in TFTR [13].

Thus, at least in principle, our approach can be extended to cover several different aspects of energy transport. This however goes beyond the scope of this paper that is to illustrate the basic properties of our family of local transport coefficients in the case of JET L-mode discharges, showing that they may constitute a valid starting point for the development of a more complete transport model.

Expressions of the diffusion coefficient that we have considered so far are:

$$\chi_{B1} = \alpha_1 \frac{|\nabla p|}{nB_0} \frac{q^3}{|\nabla q|} \tag{8a}$$

$$\chi_{B2} = \alpha_2 \frac{|\nabla T|}{B_0} \frac{q^3}{|\nabla q|} \tag{8b}$$

$$\chi_{B3} = \alpha_3 \frac{|\nabla p|}{nB_0} a\, q^2 \tag{8c}$$

We found that the global energy confinement properties and the temperature profiles resulting from transport code simulations obtained with these coefficients are rather similar. For this reason detailed results on global confinement (section 3) will refer for simplicity to χ_{B2} and the local transport properties will mainly be illustrated with χ_{B3} which does not introduce uncertainties related to the lack of an accurate experimental determination of the shear parameter.

3. THERMAL ENERGY CONFINEMENT SCALING LAW IMPLIED BY THE PROPOSED MODELS.

One can derive analytically from our models approximate expressions of energy confinement scaling laws valid for steady state, sawtooth free conditions.
Assuming that, in a single-fluid plasma, the dominant loss term in the energy balance is due to the local heat flux, and neglecting effects related to plasma elongation, one has for a coefficient of the form $\chi = f\, \nabla T$:

$$Q = - f\, n\, (\nabla T)^2 \tag{9}$$

Integrating over the plasma volume one obtains in steady state:

$$\nabla T \propto (P_{net} / r R n f)^{1/2}. \quad (10)$$

Here P_{net} is the total net input power, i.e. volume sources minus volume losses (corresponding to the thermal power flow in ref. 5) , within the plasma volume limited by the flux surface corresponding to r.

Thus in steady state all of eqs. (8) approximately imply, neglecting profile effects:

$$\chi \propto q [(a / B_0) (P_{net} / r R n)]^{1/2}. \quad (11)$$

The thermal energy confinement time τ_{Eth} is proportional to $a^2<\chi^{-1}>$, where < > denotes a properly weighted volume average [14]. In the absence of sawtooth activity, we shall therefore have approximately:

$$\tau_{Eth} \propto (B_0 R n / P_{net})^{1/2} a^2 / q \quad (12)$$

or equivalently:

$$\tau_{Eth} \propto R^{3/2} I P_{net}^{-1/2} n^{1/2} B_0^{-1/2} \quad (13)$$

The main apparent discrepancy between eq. (13) and global energy confinement scaling laws derived from the statistical analysis of global confinement experimental data is in the toroidal field dependence, which is moderately unfavourable in eq. (13) while it is non existent or moderately favourable in empirical scaling laws such as Goldston [7] and ITER89 [8] (that were derived by fitting measurements of the total rather than the thermal energy content, and using experimental data affected to a varying extent by sawtooth activity, change in power deposition profiles and hydrogen depletion due to impurities).

This may be an indication that the proposed local energy transport model requires some improvement. For example a dependence of the function F on a combination of parameters like β and ν^* (e.g. $(\beta^2\nu^*)^{1/4}$) was proposed in ref. [5].

However one has to consider that possible experimental correlations between variables (in particular n and B_0), the fact that B_0 does not vary over a wide range in the available data basis, the effect of sawtooth activity (that for the same

current favours a higher toroidal magnetic field), and the difference between total and thermal energy content, introduce a degree of uncertainty in the determination by linear regression analysis of the exponent of B_0 in empirical scalings for the thermal energy replacement time.

The favourable dependence of τ_{Eth} on the plasma density in eq. (13) is consistent with results of the analysis of the thermal energy replacement time in the Tokamak L-mode regime [15],[16].

Note finally that the relationship $\tau_{Eth} \sim <\chi^{-1}>$, using eq. (9), will imply for our models an integral of 1/q thus leading to τ_{Eth} increasing with l_i, as observed experimentally [9]. A quantitative check of this property has been carried out by means of simulations of the results of JET current ramp experiments (see next section).

Numerical tests have been performed in order to verify that the scaling law given by eq. (13) is indeed found in transport code simulations using the proposed coefficients. In fig. (1) we have summarized results obtained with model χ_{B2}, for parameters typical of L-mode plasmas in JET. Results with the other coefficients are similar. The effect of variations in input power, plasma current and (for I=3MA) plasma density are illustrated, and are in good agreement with the analytical expressions (13).

The effect of sawteeth is similar to that of an additional energy loss increasing as the safety factor q_a at the plasma boundary decreases, and depending (for a given power deposition profile), on the amplitude and frequency of sawteeth.

This loss can noticeably modify the scaling of the energy replacement time.

For example, fig. (2) shows how, for a given toroidal field B_0 =3.4 T, the scaling of the thermal τ_{Eth} with current can be significantly reduced at high current with respect to the one predicted by eq.(13), when transport is increased in the region $q<1$ to simulate the effect of sawteeth. This result is consistent with what is experimentally observed in JET discharges with $I_p \geq 5$MA [17].

Sawteeth can also affect the energy replacement time scaling with the toroidal field B_0, as mentioned above. Fig. (3) shows how, at fixed current and density, the toroidal field dependence expected from our coefficient in the sawtoothless case

($\tau_{Eth} \sim B_0^{-1/2}$) can disappear altogether as a result of an additional sawtooth-related loss of energy confinement. For any comparison between values of τ_{Eth} predicted by eq. (13) and experimental observations, the measured thermal energy should be used in the definition of τ_{Eth}, and the effects of sawtooth activity and the heating efficiency should be (at least approximately) taken into account [14],[18]. In addition, only steady state cases should be considered.

Such a comparison has been done by means of the interpretative code FALCON and is shown in fig. (4), that compares τ_E from eq. (13) (with a numerical coefficient equal to 0.23, when s, m, MA,MW, T and $10^{20} m^{-3}$ are used), with the estimates of the same quantity obtained by the FALCON code for a series of JET discharges in the range 1-7 MA at toroidal field $B_0 > 2.8$ T.

Fig. (5) shows the results of the comparison between the same estimates of the thermal energy confinement and the global energy confinement time predicted by the ITER89 scaling law [8]. The deviation of the predicted values from the experimental ones in this case has to be expected and illustrates essentially that somewhat different quantities are compared in this figure.

4. SIMULATIONS OF LOCAL TRANSPORT IN JET DISCHARGES.

As observed in section 2, the empirical transport coefficients given by eqs. (9) are composed by ingredients that are compatible with results of local as well as global energy transport analysis of L-mode discharges in JET and other devices [5], [6], [9] ,[10] ,[13]. Here we test quantitatively, by means of simulations of experimental results in JET, the local transport properties of the coefficients.

This requires to specify in more detail the model to be used. We have 'completed' our models by assuming $T=T_e$, $n=n_e$ and $p=p_e$ in eqs. (8). In addition we assume $\chi_i=\chi_e$.

These assumptions are by no means uniquely determined: they are instrumental to an initial study of the basic local properties of our Bohm-type coefficients, but we are aware that they may not be consistent with the entire variety of regimes and results observed in JET and other devices; further development of the model is likely to be required, for example by introducing $\chi_i \neq \chi_e$.

As a transport code to test our coefficients we have used the 1-1/2D JETTO code,which is linked to the experimental profile data basis available at JET. The code has been operated in a semi-interpretative way, by using prescribed profiles of density, Z_{eff}, radiated power and power deposition profiles of auxiliary heating and solving the electron and ion energy conservation equations toghether with the equation for the evolution of the q profile, assuming neoclassical resistivity.

The computations required to test numerically the global confinement scaling properties of our coefficients have been performed assuming a shape of those profiles that are prescribed similar to the shape observed experimentally in the range of parameters considered. In these cases the equilibrium configuration, computed initially, has been kept fixed in time for each simulation.

For the simulation of real JET discharges, the profiles prescribed have been taken from the JET data basis, to which the JETTO code is linked, using the same profiles as in the interpretative code TRANSP when possible. Moreover the time evolution of the equilibrium configuration has been followed by solving the MHD equilibrium equation with the computed p and q profiles, and imposing experimental values of the poloidal flux as boundary values.

As we have observed the properties of the coefficients given by eqs (9) are similar, particularly for steady state or relatively slowly evolving discharges as those considered here.

In fact $q/(|\nabla q|\ a)$ does not vary much ($\approx\pm 30\%$) over most of the plasma cross section in steady state cases.The same is true for $|\nabla T| / (|\nabla p|/n)$.

As an example of this we show in fig. (6) the electron temperature profiles computed with the three coefficients given by eqs (8) in the case of a typical steady state JET L-mode discharge at I=3.27 MA , B_0=2.8 T. The results of the three models are all within the experimental error bars in the so called transport dominated region ($q>1, r/a<0.9$) where meaningful tests can be carried out without taking into account an accurate description of sawtooth activity and atomic physics processes . Given the scope of this work no attempt is done to validate any of the models outside this region.

The results presented in the following have been obtained with the coefficient χ_{B3}, which is the simplest to test, particularly in time dependent situations,

because it does not imply uncertainties related to the determination of the shear parameter. The coefficient $\alpha_3=3.3\cdot10^{-4}$ (SI units and eV) was determined numerically from the simulation of a few steady state L-mode discharges in the range 1-5 MA.

4.1. ρ^* Scaling Experiments

We consider first the simulation of discharges that were obtained in JET for the scaling of transport with the normalized Larmor radius ρ^* [6].

In this case the plasma current, the toroidal magnetic field, the density, the power level and the power deposition profiles chosen in the experiments aimed at varying only ρ^*, while keeping all other non dimensional parameters unchanged in different discharges. The experimental results have been shown in [6] to favour an interpretation in terms of a Bohm type local transport. Therefore, one expects our model to be successful in simulating these discharges. This is indeed the case as illustrated in fig. (7) and (8). Fig. (7) shows a comparison of computed and experimental electron temperature profiles for two discharges at 2 MA,1.7 T and 4 MA, 3.4 T at times when quasy steady state is reached in both discharges. Figs. (8a) and (8b) show the time evolution of the ratio between the experimental and the computed values of T_e at R=3.4 m, R=3.6 m and R=3.8 m for the same discharges. These radial positions have been chosen to avoid uncertainties in the comparison related both to sawtooth activity close to the magnetic axis and atomic physics phenomena and the influence of boundary conditions close to the plasma boundary.

4.2. Current Ramp Experiments

The simulation of current ramp experiments in JET [9] is a test of the dependence of our transport model on the local safety factor q, or equivalently on the current density distribution across the plasma column. This determines the dependence of the thermal energy confinement time upon the internal inductance l_i and the total plasma current, which is important for extrapolations to ITER. It is a typical example of the importance of specifying the correct q dependence of the function F in the expression (2).

The simulations have been carried out for both cases of current ramp up and ramp down, the plasma current being respectively increased from 1.5 MA to 3 MA or decreased from 3 MA to 1.5 MA.

The simulation of the time evolution of the equilibrium configuration is important for these experiments because the plasma shape varies as the current is increased or decreased, as illustrated for the current ramp down case by fig. (9a) and (9b), showing the magnetic flux surfaces computed by the JETTO code at the beginning and the end of the ramp.

Fig. (10) compares the computed and experimental time evolutions of the thermal electron energy content in the two cases. The corresponding evolution of the electron temperature profiles is given in Figs. (11) and (12).

These results show that the predicted linear dependence of the thermal energy content on current when a steady state is reached and on the current density distribution (i.e. l_i) during the current evolution, are in agreement with experimental observations.

4.3. On-Axis and Off-Axis Heating Experiments

As a further test of the model we consider the simulation of the temperature evolution of a discharge with off-axis heating as compared to one with on axis heating [10]. The two discharges have similar current $I_p \approx 3$MA, toroidal field $B_t \approx 2.8$T, average electron density $\langle n_e \rangle \approx 3 \cdot 10^{19}$ and ICRH input power $P_{aux} \approx 10$ MW. The ICRH power deposition profiles to electrons and ions stored in the JET data basis and used in the simulations are compared in figs. (13) and (14) at times close to the beginning of the auxiliary heating . They do not change significantly throughout the heating phase of each discharge.

Figs. (15) and (16) show a comparison of computed and experimental electron temperatures at three different times following the onset of additional heating in the two discharges. Again the results of our simulations agree with experimental observations.

Fig. (17) shows a comparison of the thermal diffusivity χ_e in the two cases towards the end of the heating phase. One notices that χ_e tends to increase with

the power deposited to the electrons as a result of its dependence on $|\nabla T_e|$. This contributes to the "resilience" of the electron temperature profiles.

This effect might play a role also when a significant amount of power is radiated over a region that extends significatively inside the plasma. Because of the dependence on $|\nabla T_e|$, our diffusivity coefficient is reduced at a given radius as the total net input power, i.e. the input power minus the radiated power, inside that radius decreases. This would limit the effect of radiation losses on the energy replacement time, a prediction of our model which could be tested experimentally, e.g. by injection of a small amount of high-Z impurities into the edge of a low-radiation plasma.

5. CONCLUSIONS

We have identified empirically a family of local energy transport coefficients of the Bohm type characterized by simple functional dependences on few plasma parameters, and capable of reproducing several features of energy confinement as observed in JET L-mode discharges.

We have shown that these local transport coefficients determine a dimensionally correct scaling of the thermal energy confinement time with the so called "engineering" parameters that is compatible with that inferred from experimental data in the L-mode regime.

Tests with a 1 1/2D predictive transport code show that these coefficients lead to temperature profiles agreeing in shape and time evolution with experimental observations in the case of relevant JET discharges, such as ρ^* scaling, current ramp and off-axis heating experiments.

Potentially the proposed family of models can be tailored and extended to include features that might allow to simulate regimes other than the L-modes. However this will require much more theoretical, computational and experimental work: to a large extent, a complete transport model is some way off even for L-modes.

Most uncertainties are related to the fact that in our empirical approach the experimental error bars are usually large enough to prevent a clear-cut choice being made between dimensionally equivalent local parameters such as $\nabla T/T$ and $\nabla p/p$. The uncertainties become even larger when a quantity such as the

shear length is included in the model. The problem of the relative importance of electron and ion heat transport also remains open.

We did not tackle these problems in this paper, limiting ourselves to the study of the basic properties of our family of models. These properties seem to us interesting enough to constitute a valid basis for further work in this field. In particular, these models are sufficiently complete to carry out predictive computations, e.g. for ITER, and to make comparisons with predictions based on models of the gyro-Bohm type such as the Rebut-Lallia-Watkins model [12].

Our results also highlight the importance of performing dedicated experiments, preferably in machines of different size, aiming at determining the dependence of the transport model on those non dimensional quantities such as q,β and ν^* that may be relevant to determine the dependence of the thermal energy confinement on "engineering" parameters such as I,B_0 and R. The existing empirical global confinement scaling laws, derived from regression analysis on data from multi-machine data basis but including many effects not directly related to the underlying local energy transport mechanism (e.g. confinement of non thermal particles, sawtooth activity and heating efficiency) are a valuable guideline, but need to be supported by more specific information on what determines them.

REFERENCES

[1] Kadomstev B B, 1975 Sov. J. Plasma Phys. 1 295.

[2] Connor J W and Taylor J B, 1977 Nucl. Fusion 17 1047.

[3] Christiansen J P et al , 1991 Nucl. Fusion 31 2117.

[4] Waltz R E et al 1990 Phys. Rev. Lett. 65 2390.

[5] Perkins F W et al , 1993 Phys. Fluids B 5 477.

[6] Christiansen J P et al, 1993 "The Scaling of Transport with Normalized Larmor Radius in JET", JET-P(93) 16, to appear in Nuclear Fusion.

[7] Goldston R J , 1984 Plasma Phys. Contr. Fusion 26 87.

[8] Yushmanov P N et al, 1990 Nucl. Fusion 30 1999.

[9] Challis C D et al , 1992 Nucl. Fus. 32 2217.

[10] Cordey J G et al, 1992 Proceedings of the 14th Int. Conf. on Plasma Physics and Controlled Nuclear Fusion Research, IAEA-CN-56/D-3-4,Wurtzburg 1992, IAEA, Vienna.

[11] Neudatchin S V , Cordey J G and Muir D G, 1993 Proc. 20th Eur. Conf. on Controlled Fusion and Plasma Physics, Lisboa 1993, EPS, Vol I p. 83.

[12] Rebut P H , Lallia P P and Watkins M L, 1989 in Plasma Phys. and Contr. Nucl. Fus. Res. 1988 (Proc. 12th Int. Conf. Nice, 1988), Vol.2, IAEA, Vienna p. 191.

[13] Zarnstorff M C et al , 1991 in Plasma Phys. and Contr. Nucl. Fus. Res. 1990 (Proc. 13th Int. Conf. Washington, D.C., 1990), Vol.1, IAEA , Vienna p. 109.

[14] Callen J D et al , 1987 Nucl. Fusion 27 1857.

[15] Johnson D W et al, 1990 Proc. 17th Eur. Conf. on Contr. Fus. and Plasma Phys., Amsterdam 1990, EPS, Vol I p.114.

[16] Kikuchi M et al, 1992 Proc. 14th Int. Conf. on Plasma Phys. and Contr. Nucl. Fus. Res., IAEA, Wuerzburg 1992, paper IAEA-CN-A-3-3.

[17] Lomas P J et al, 1992 Proc.14th Int. Conf. on Plasma Phys. and Contr. Nucl. Fus. Res., IAEA, Wuerzburg 1992, paper IAEA-CN-A-3-2.

[18] Chang Z and Callen J D, 1990 Nucl. Fusion 30 219.

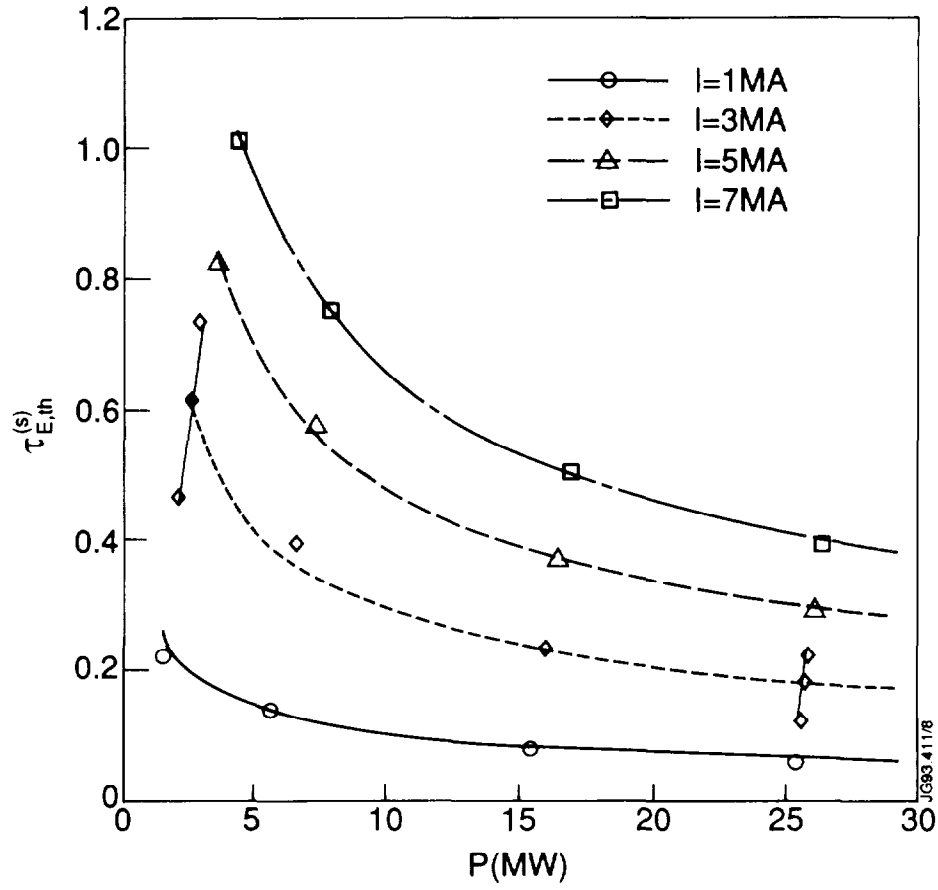

Fig.1: τ_{Eth} as a function of P predicted using χ_{B2} without sawteeth enhanced transport for various values of the plasma current and density. The points represent the results of local transport simulations of idealized JET discharges. The lines are $P^{-1/2}$ power laws passing through the highest power points, while the 'bending error bars' on the 3MA curve correspond to cases where the density has been varied by a factor of 3.

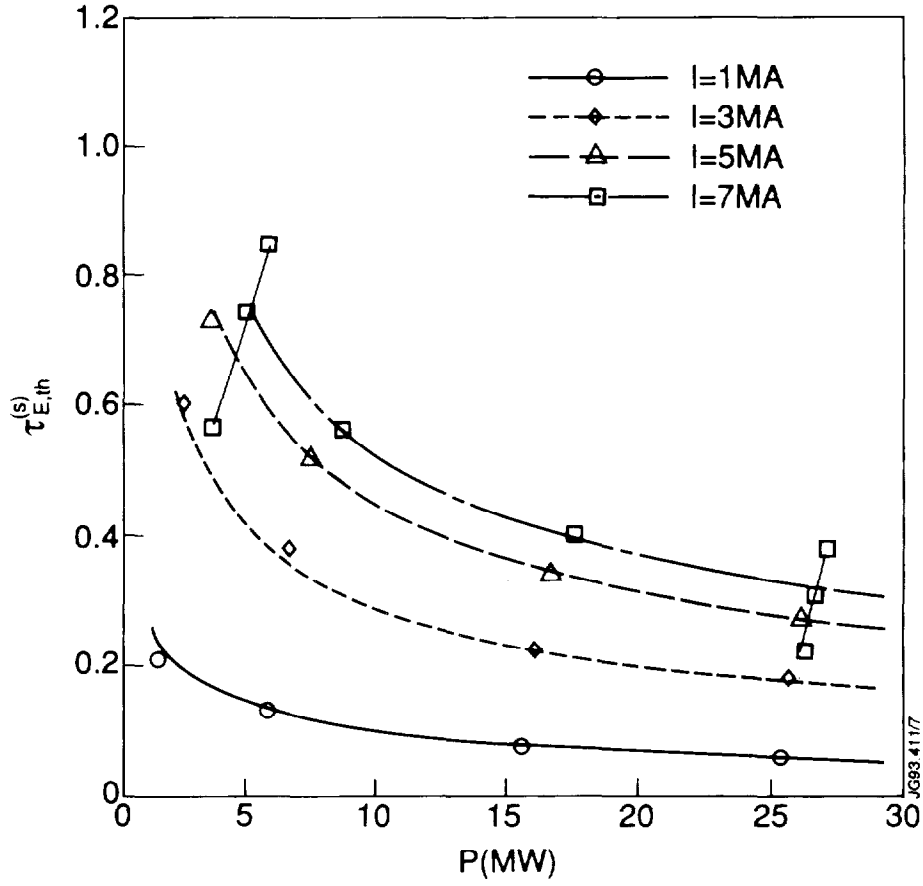

Fig.2: τ_{Eth} as a function of P predicted using χ_{B2} with sawteeth enhanced transport for various values of the plasma current and density. The points represent the results of local transport simulations of idealized JET discharges. The lines are $P^{-1/2}$ power laws passing through the highest power points, while the 'bending error bars' on the 7MA curve correspond to cases where the density has been varied by a factor of 3.

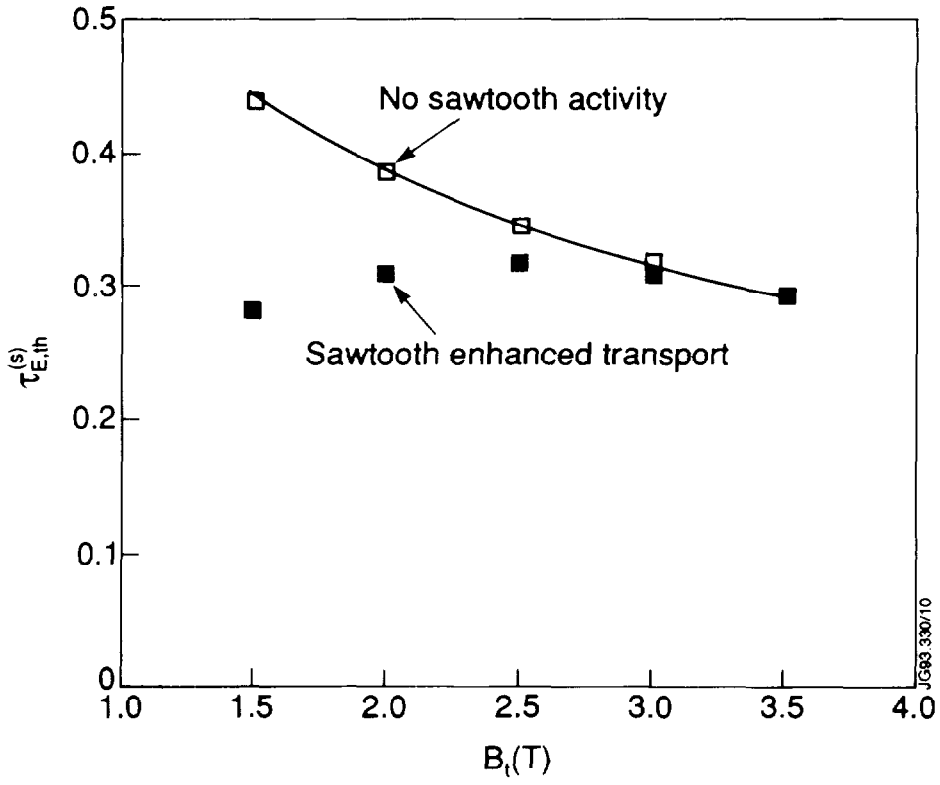

Fig.3: τ_{Eth} as a function of B_t predicted using χ_{B3} with and without sawteeth enhanced transport. The points represent the results of local transport simulations of idealized JET discharges. The line represents the $B_t^{-1/2}$ power law passing through the highest toroidal field point.

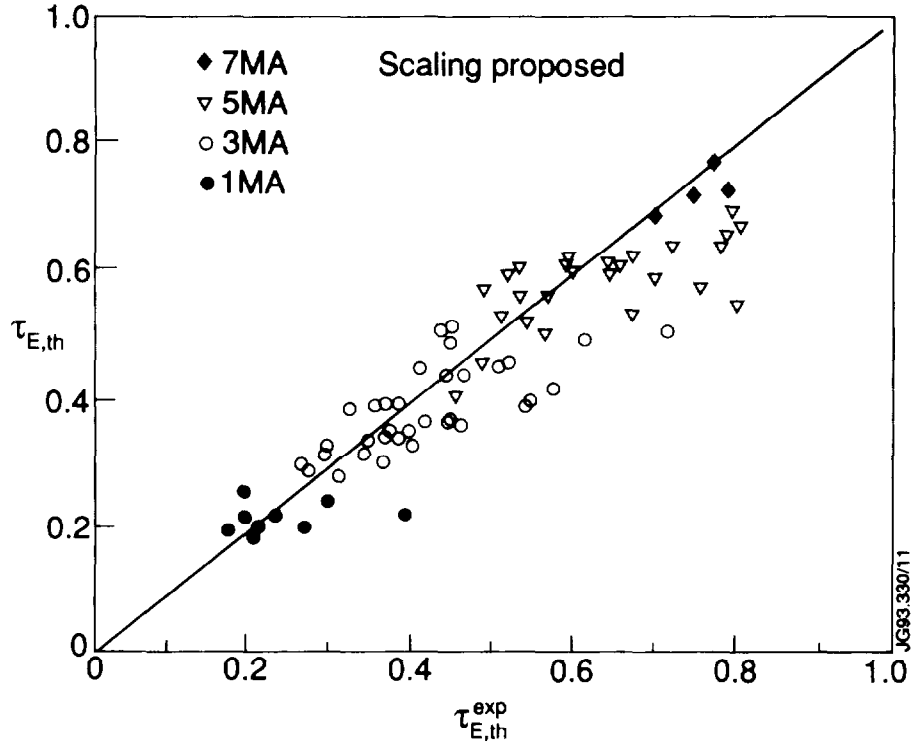

Fig.4: τ_{Eth} predicted by our scaling compared to 'experimental' ones for JET shots at various currents (B_0>2.8T).

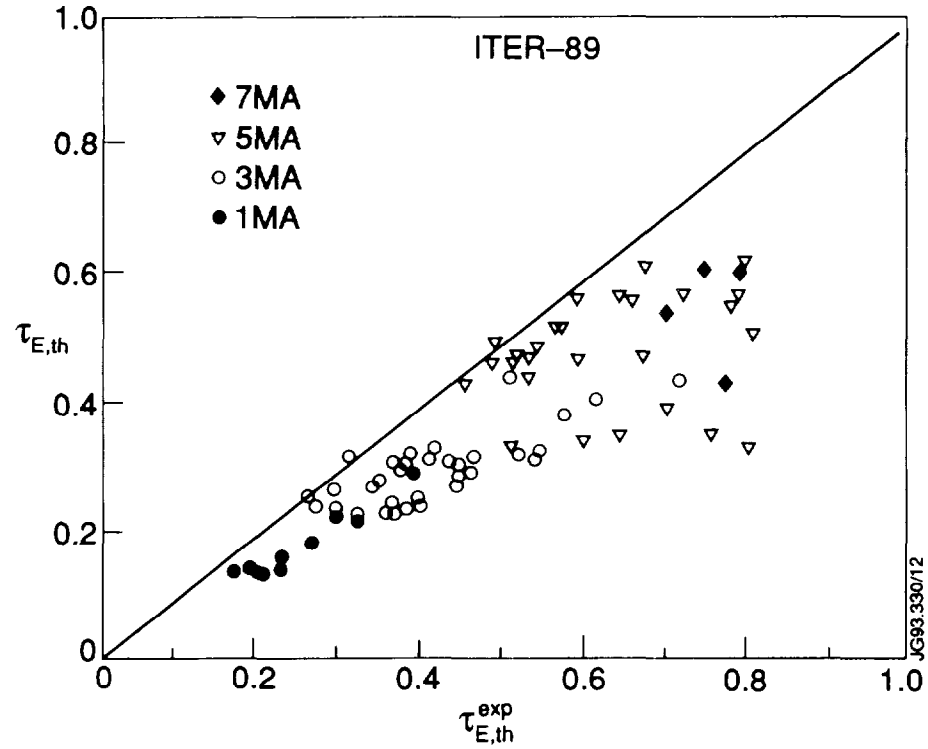

Fig.5: τ_{Eth} predicted by ITER89 scaling compared to τ_{Eth} 'experimental' values for JET shots at various currents (B_0>2.8).

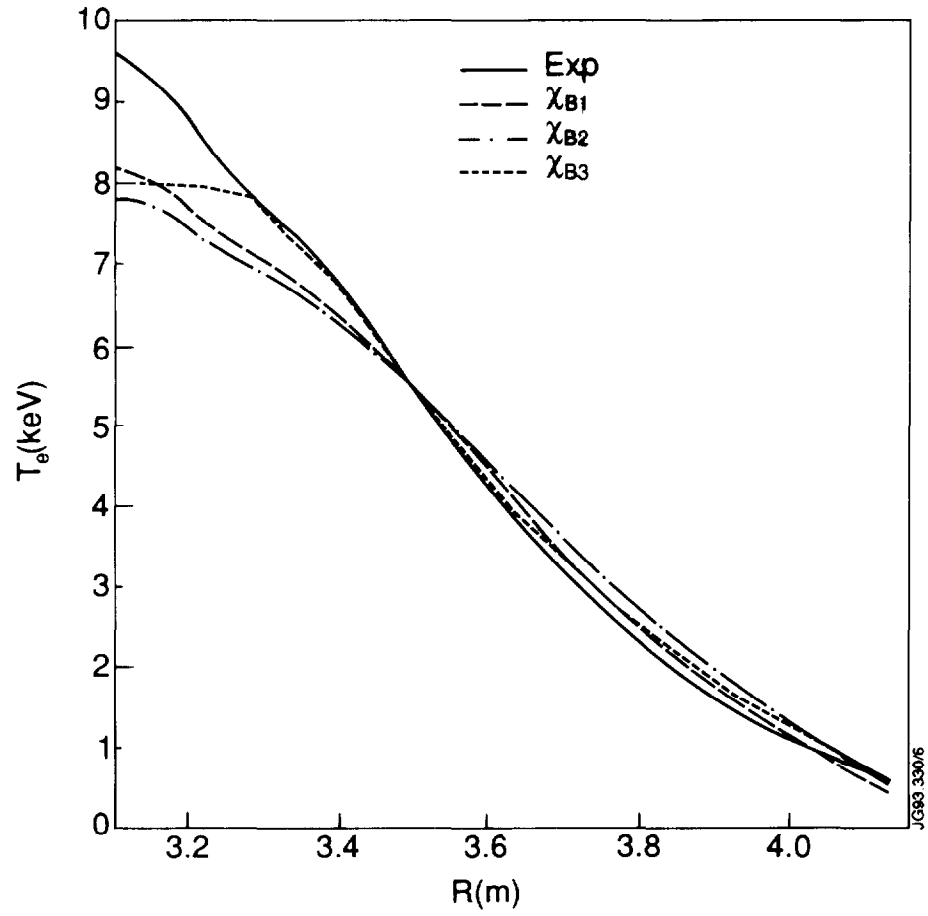

Fig.6: Experimental T_e profiles compared with those computed with χ_{B1}, χ_{B2} and χ_{B3} for a typical JET L-mode case.

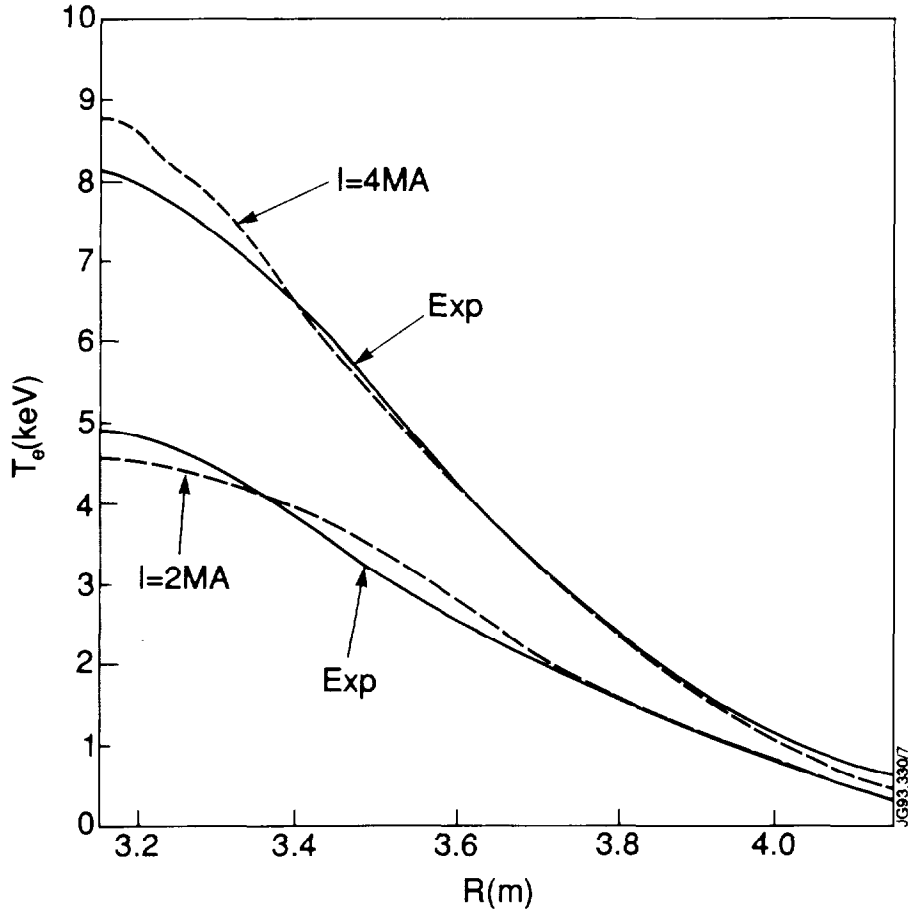

Fig.7: Simulated and experimental T_e profiles for two discharges of the ρ^* scaling experiment at JET.

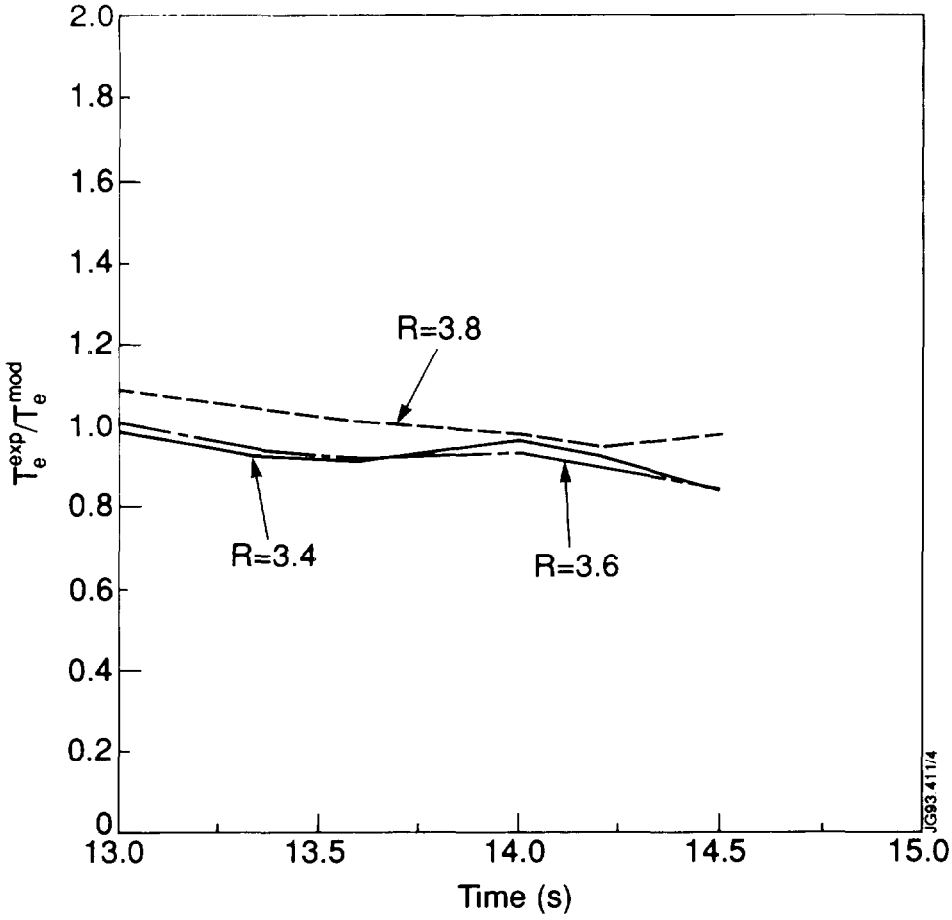

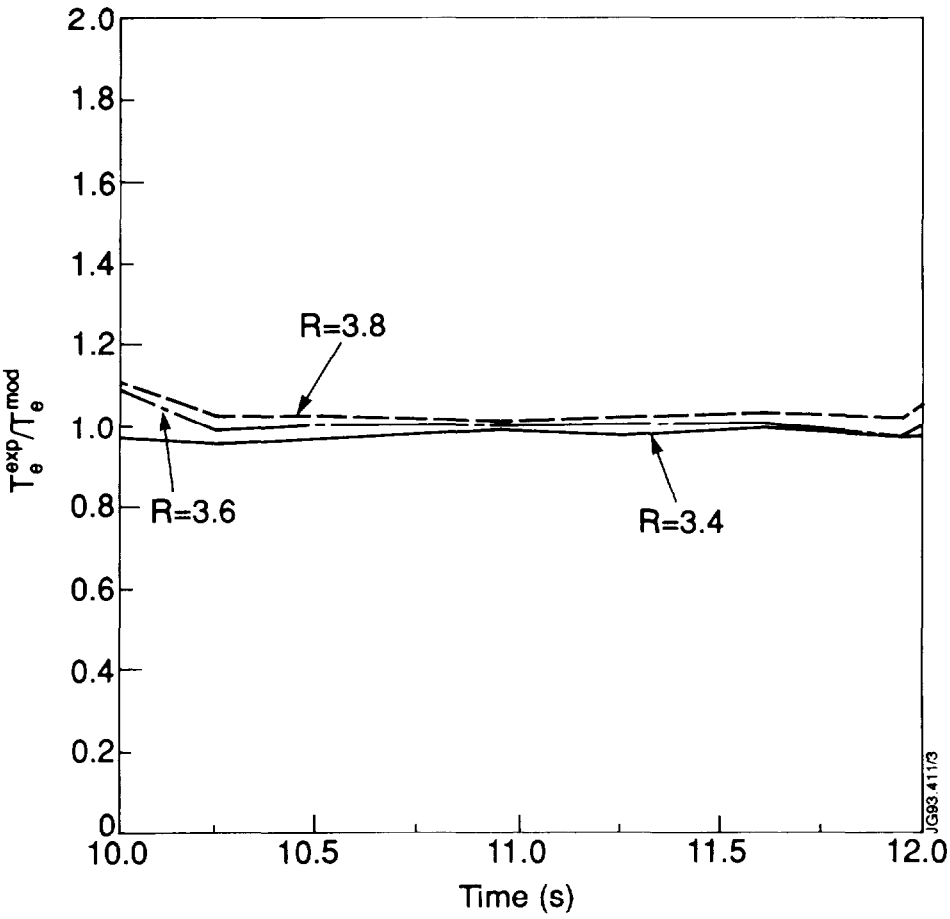

Fig.8: Time evolution of the ratio of experimental and simulated electron temperatures at different radial locations for the 2MA a) and 4MA b) discharges of the ρ^* scaling experiment at JET.

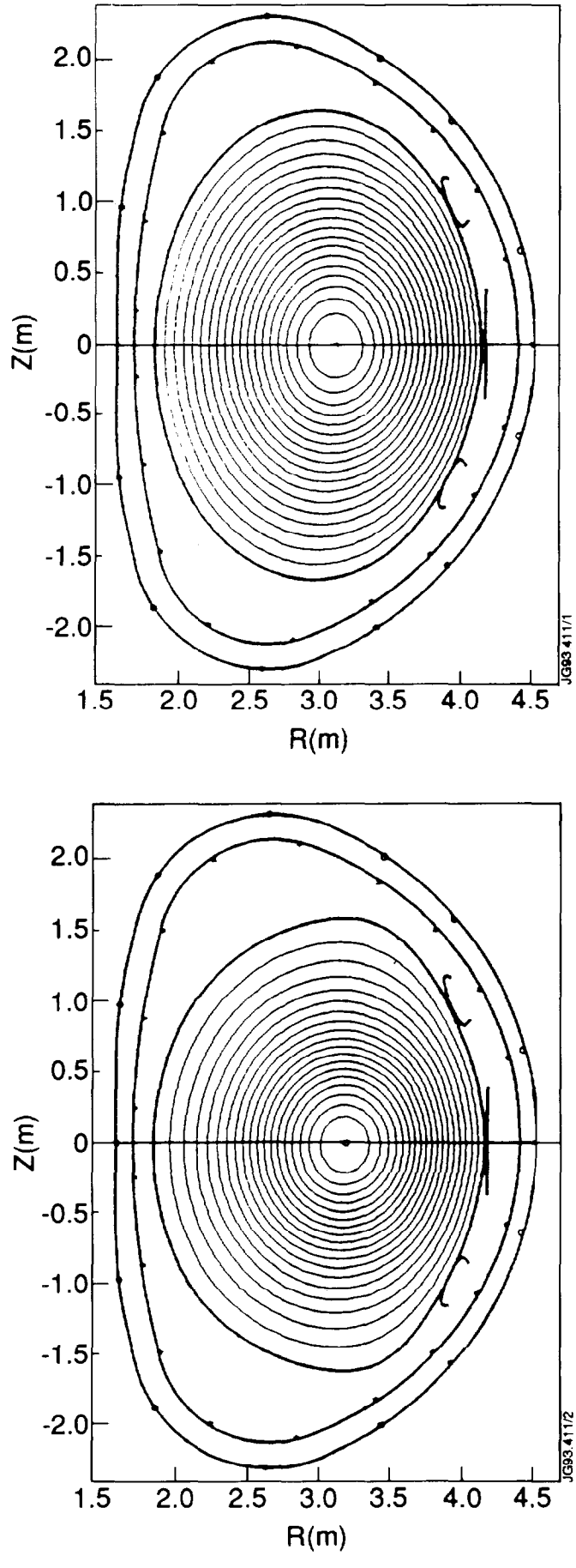

Fig.9: Poloidal cross section of magnetic flux surfaces for the current ramp down JET experiment at the beginning a) and at the end b) of the ramp.

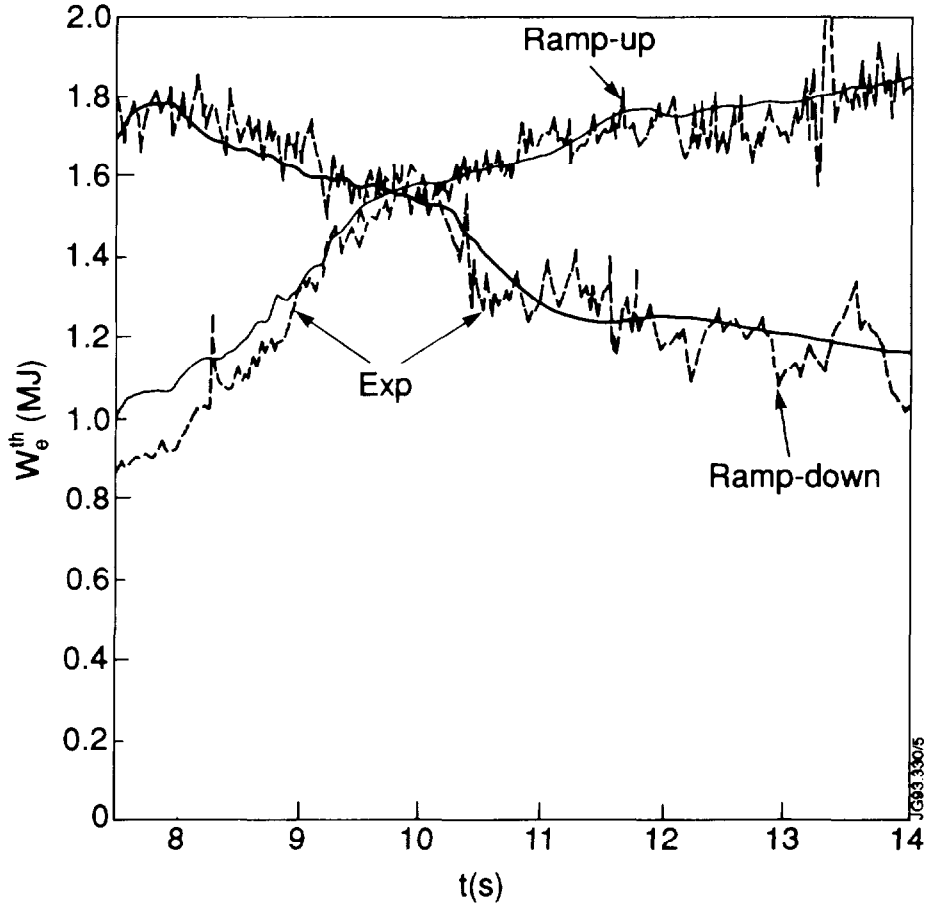

Fig.10: Simulated and experimental time evolution of the electron thermal energy content for JET current ramp experiments.

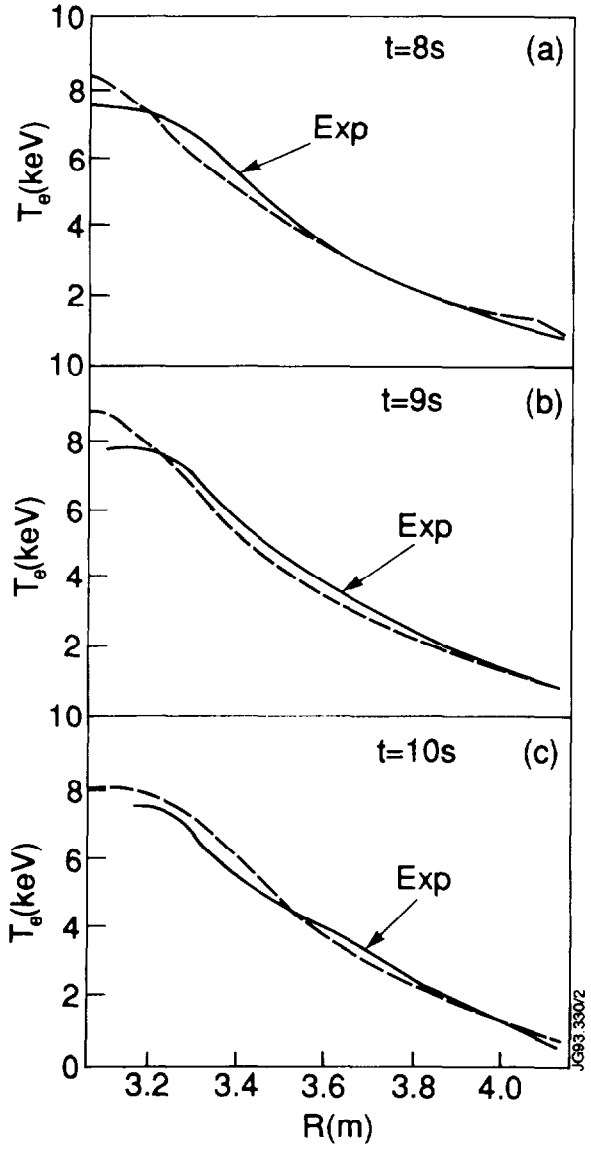

Fig.11: a, b, c Time evolution of simulated and experimental T_e profiles for the current ramp-down case.

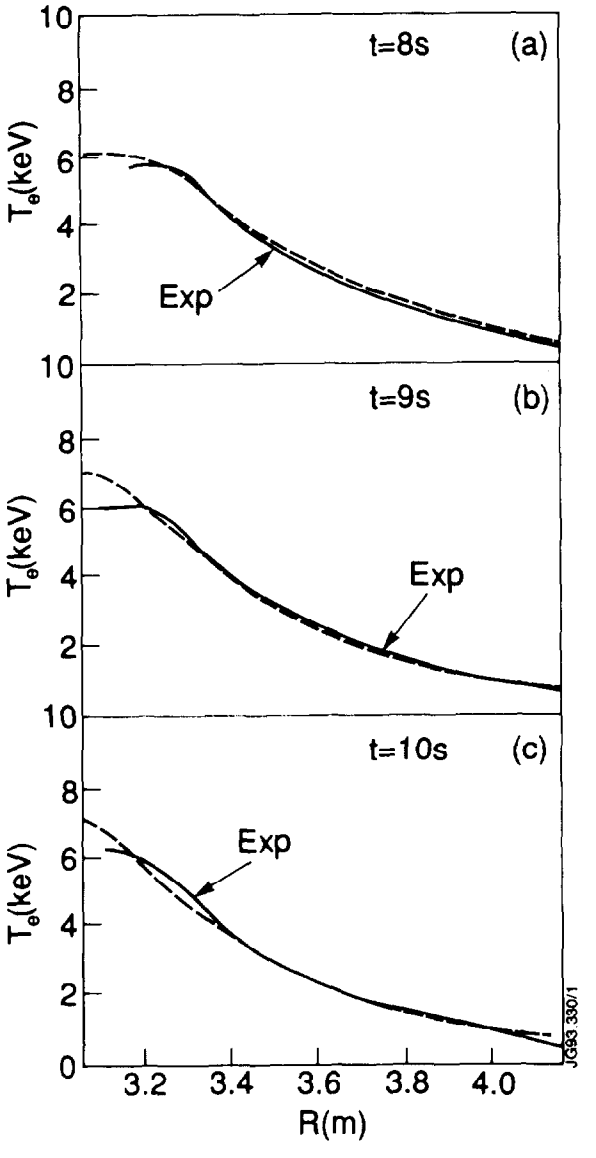

Fig.12: a, b, c Time evolution of simulated and experimental T_e profiles for the current ramp-up case.

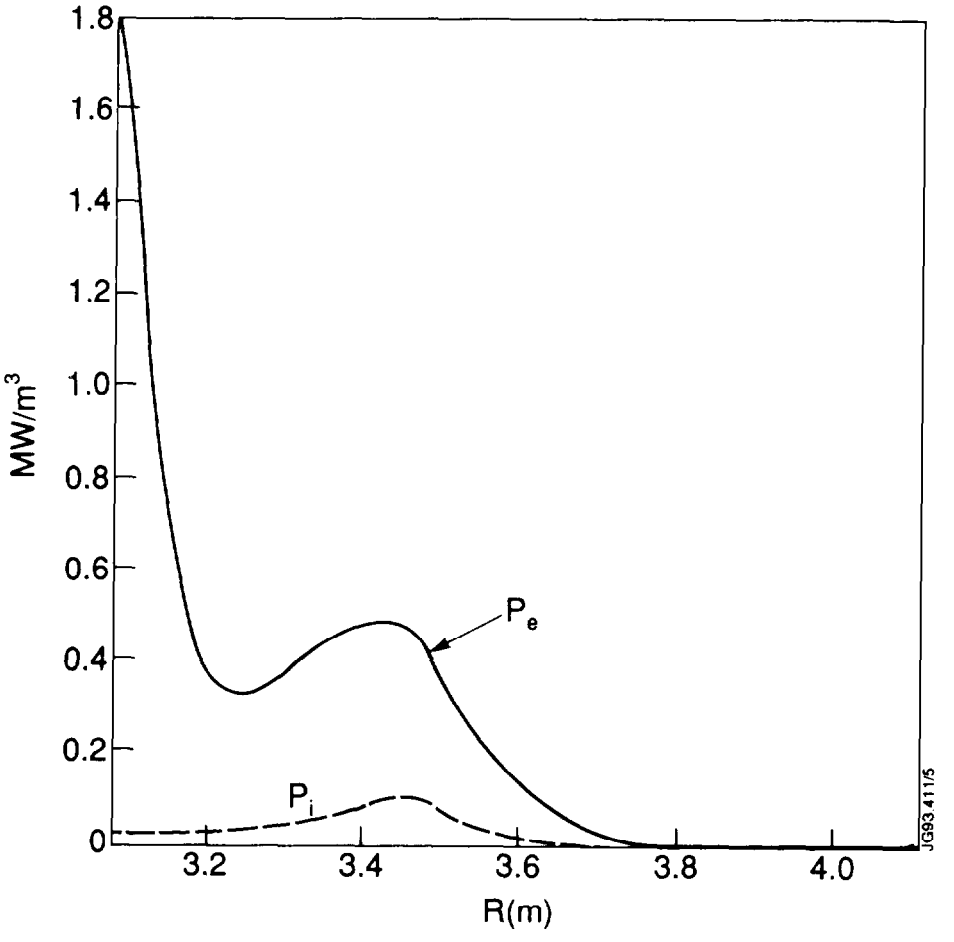

Fig.13: Electron and ion auxiliary power deposition profiles for the on-axis heated discharge.

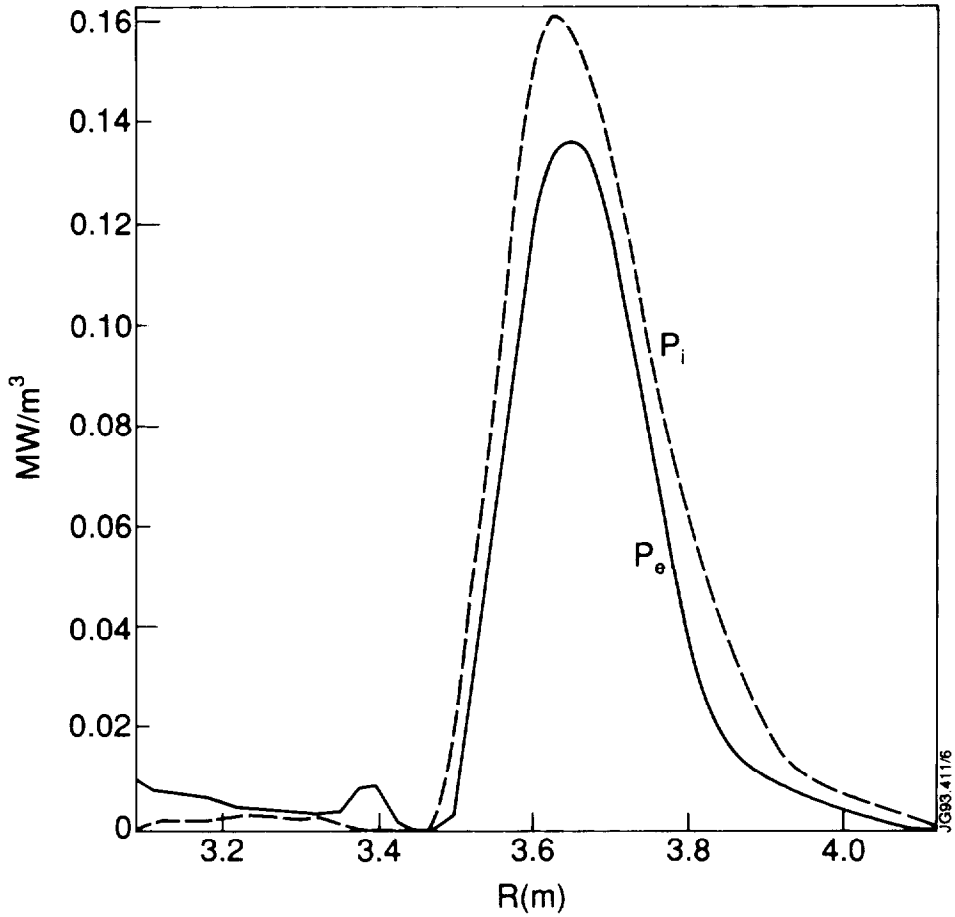

Fig.14: Electron and ion auxiliary power deposition profiles for the off-axis heated discharge.

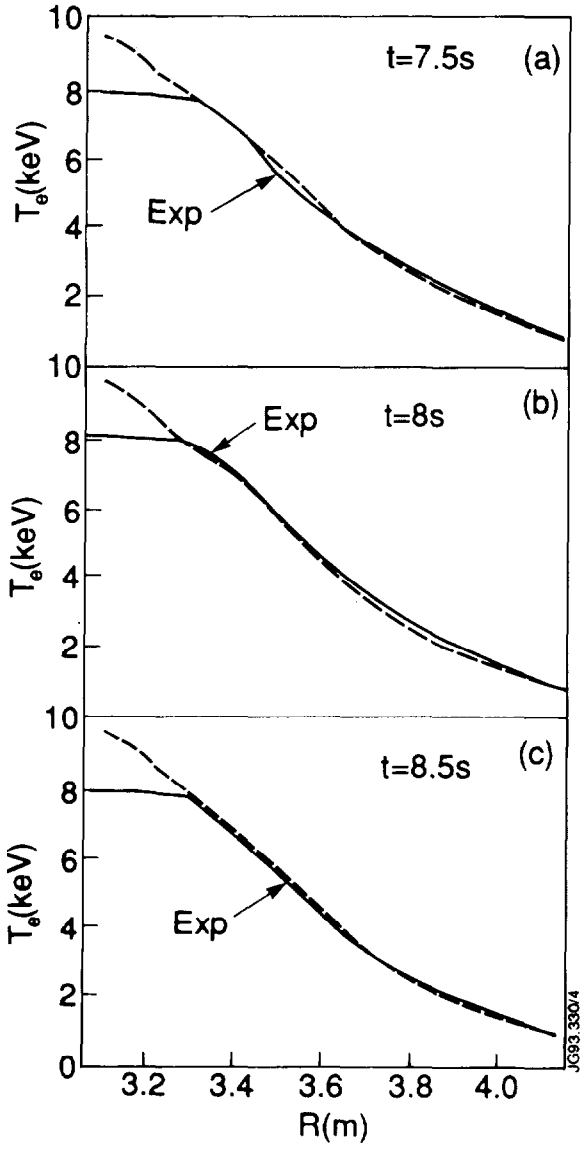

Fig.15: a, b, c Time evolution of simulated and experimental T_e profiles for the on-axis heated discharge.

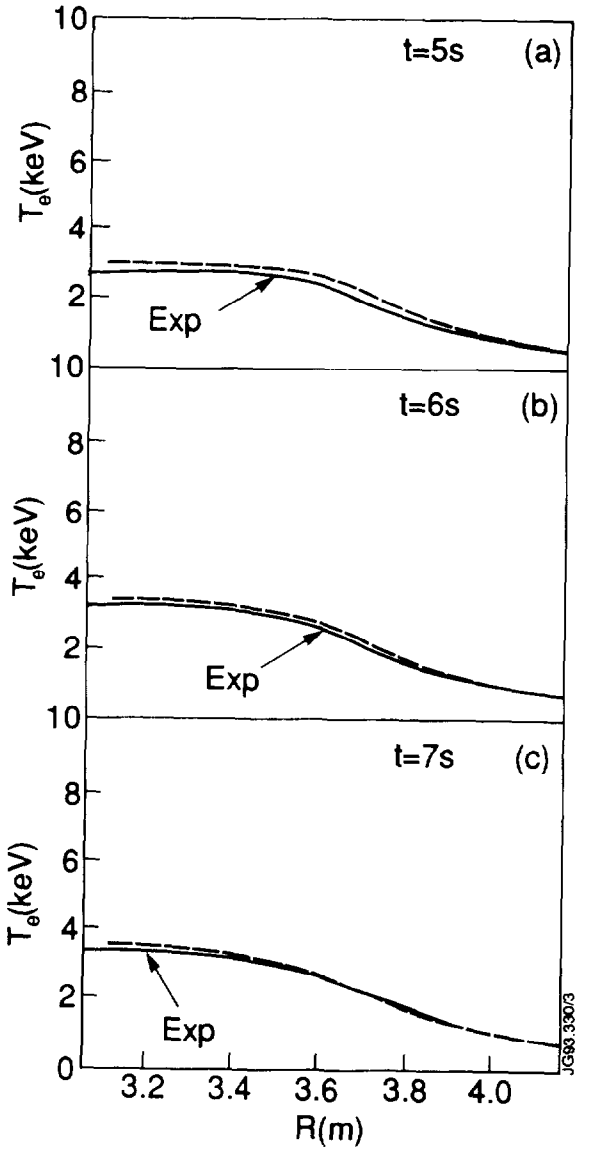

Fig.16: a, b, c Time evolution of simulated and experimental T_e profiles for the off-axis heated discharge.

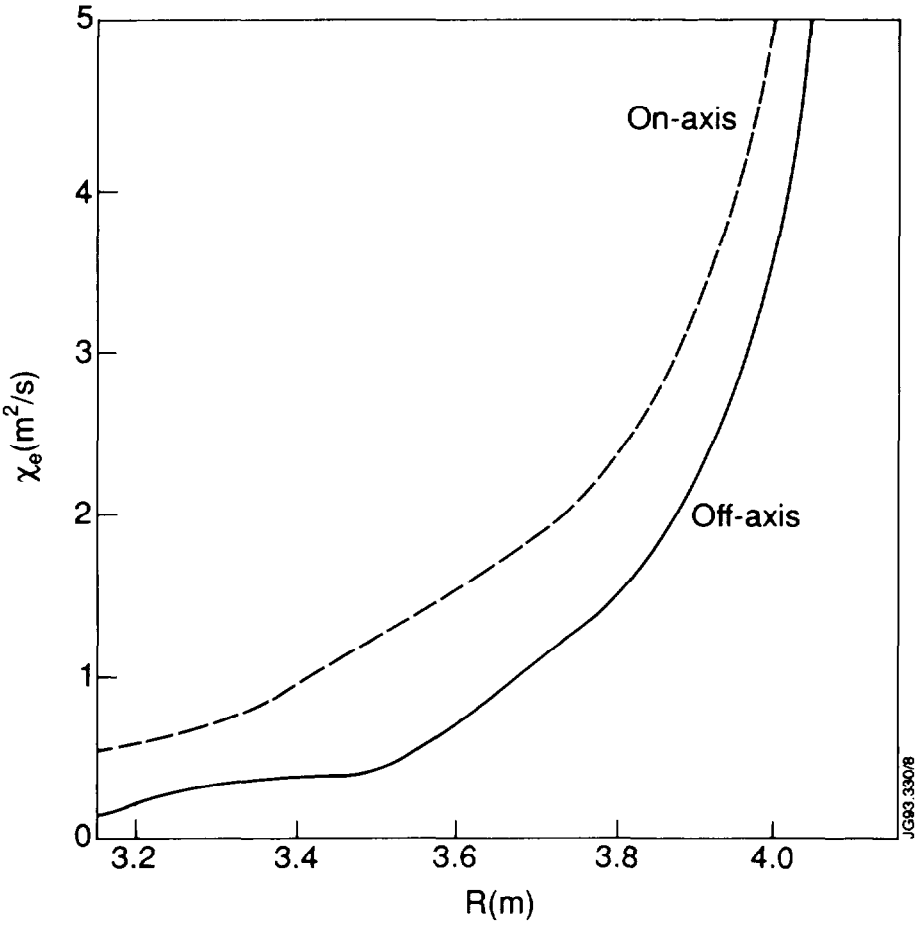

Fig.17: Comparison of the thermal diffusion coefficient profiles for the on-axis and off-axis heated discharges.